Optical Absorption Based Transducer Enabled Optical Fiber Refractive Index Sensor Operating at the Temperature Range of 10ºC to 60ºC

Dr. S. Venkateswara Rao[1] & S. Srinivasulu[2*] , S. Srinivasulu[*]

[1]Professor of Physics, Department of Physics, College of Engineering Hyderabad, J N T University Hyderabad, Telangana State, India.

[2]UGC–Senior Research Fellow, Department of Physics, College of Engineering Hyderabad, J N T University Hyderabad, Telangana State, India.

ABSTRACT:

Several transducers have been demonstrated to determine the refractive index of liquids either dark or transparent in the past few decades. In the present work a novel optical absorption based U-shaped glass probe sensor has been developed to study the refractive index of various liquids in the temperature range between 10ºC to 60ºC using Toluene and Acetonitrile mixtures at a source wavelength of 660nm. The sensitivity of the sensor also studied, by increasing the length of interaction between the light transmitting through the U-shaped glass rod and the analyte at the region of the sensing. The variation of the output power was observed to be a function of the optical absorption related change in refractive index of the analyte around the glass rod. The output power data related to different interaction lengths reveals that, as the length of interaction increases, the output power decreases. The investigation on temperature dependent variation of refractive index was carried out, and the results show that higher is the temperature of the active medium around the glass rod, lower is the refractive index and hence greater is the output power. The sensor is calibrated with respect to refractive index and output power at operating range of temperatures between 10ºC and 60ºC. With the help of this sensor a response time as short as the measurement precision of the order of 8×10^{-6} can be obtained.

Keywords: Acetonitrile, Active medium, Analyte, Refractive index, Source wavelength of 660nm, Toluene, U-shaped glass probe sensor.

INTRODUCTION:

Considerable interest has been attracted towards the development of optical fiber refractive index sensors in the past few decades. Initially the optical fibers were mainly used for communication purpose across the globe. During 1970's when the optical fibers were evolving for communication purposes, it was observed that the optical fiber as a light guiding medium observed to be highly sensitive to certain internal perturbations like bubbles, voids, impurities,

refractive index difference, micro structural variations, compositional variations etc. and certain external perturbations such as micro-bends, macro-bends, temperature, pressure, etc. On the observation of the sensitivity of the optical fiber for external and internal perturbations, a new thought began in the scientific world to construct numerous kinds of sensor and systems to measure several environmental parameters such as temperature, refractive index, pressure, salinity, surface structure, pH, strain, viscosity, density, chemical activity, etc., fields like electric, magnetic, etc. and so on and so forth. The initial developmental work was concentrated on the development of hydrophone, which can be used for under water applications, later on the technique was extended to the fields like industries, medical, defence, science and technology, agriculture, etc. The fiber optic sensing technique was also extended to civilian applications and was expected to play a major role in the development of sensors almost in all walks of life.

The fiber optic sensors offers various advantageous over conventional sensors, as they exhibit excellent characters, that includes electro-magnetic immunity, corrosion and erosion resistance, high precision, electrical resistance, reliability, durability, ruggedness, provision of multiplexing, chemical inertness, simultaneous measurement of parameters as OTDR and resistance to radiation fields, etc. [1]. The refractive index of liquids can be influenced by the variations in various parameters including potential of Hydrogen (pH), temperature, electric field, concentration and magnetic field, etc. [2-6]. Several kinds of refractometers have been constructed by applying various kinds of techniques, designs and principles of operations for the measurement of refractive index which include surface plasma resonance (SPR), critical angel refractometer, grating based sensors, etc. as part of conventional sensors [7-13]. However, there are many disadvantages that are to be overcome which includes complex fabrication, sensitivity in measurement of temperature, etc. The SPR refractive index sensors, though they are relatively expensive to use, they offer advantages of accuracy and response time, etc. Grating based fiber optic refractive index sensors operate with 10^{-5} to 10^{-6} resolution, operating at 1550nm are having sensing heads which are sensitive to simultaneously to temperatures. For the measurement of refractive index a double pulse calibration method was reported by Chang-Bang Kim et al in the literature [14].

EXPERIMENTAL DETAILS:

The geometry of the sensor consist of a U-shaped glass rod of specific dimensions connected between a semiconductor laser source of 660nm wavelength and a bench mark optical digital power meter employing tow insensitive plastic clad silica (PCS) fibers of 200/230µm. The U-shaped glass rod connected between two fibers acts as a clad removed (core) part of plastic clad silica fiber, whose dimensions are compatible to the dimensions of the cores of the two PCS fibers used. Therefore, when light launched from the source transmits unattenuated in the two fibers, but it attenuates along the length of the U-shaped glass rod, which acts as a core and which was not covered by any kind of cladding. Thus, the light injected from the source suffers a substantial loss during its transportation along U-shaped glass rod, which acts as a sensing zone. Along the length of the glass rod, the loss of higher order mode radiation takes place in the form of leaky radiation modes. As length of the U-shaped glass rod i.e. sensing length increases, the loss of light radiation increases. In the region of sensing the light traveling along the length of U-shaped glass rod can be made to interact with some external parameter and thus by collecting the power reaching the receiver. A relationship can be formed between the variation in the external

parameter (analyte) and the corresponding variation in the output power. The sensor with this kind of geometry wherein the light modulation is taking place outside the fiber is called extrinsic or hybrid or passive fiber optic sensor.

Takeo et al in a comparison study of various sensors have reported, an optical fiber in which a PCS fiber was bent into a U-shape, at a section of the fiber by removing the plastic cladding [15]. When bend section of the fiber was immersed in a liquid of a refractive index $n_l > n_{air}$, the output power yields a signal that is different from that with a bare fiber design.
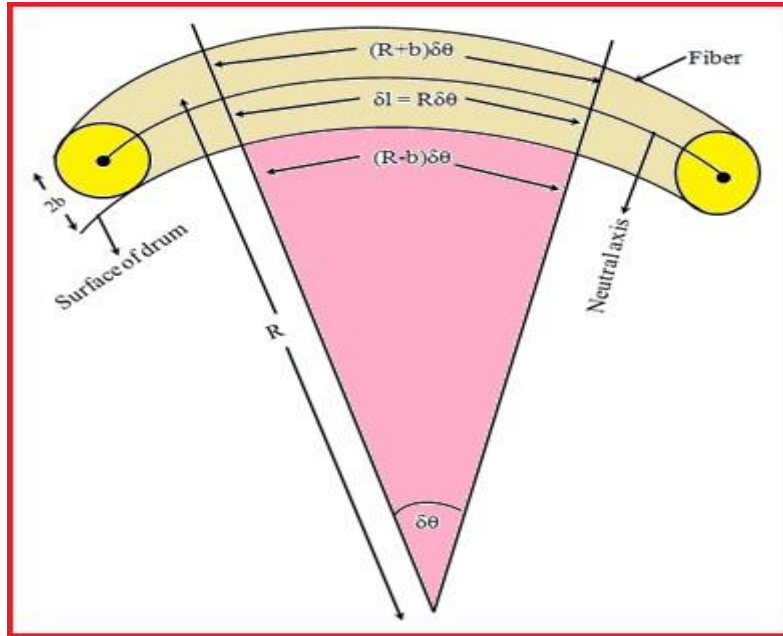

Fig.1: Surface strain produced by bending.
Strain at outer surface (tension) $= \dfrac{(R+b)\delta\theta - R\delta\theta}{R\delta\theta} = \dfrac{b}{R} =$ strain at inner surface (compression)

The loss of light during bent portion is a function of 1. Critical bending radius, 2. Thickness of the rod, 3. Bend radius of the rod, as given in the mathematical equation as
Bending loss $\propto \left[\dfrac{-R}{R_c}\right]$

Thus, the optical power loss at a major bend depends exponentially on bend radius.

$R_c = \dfrac{a}{(NA)} = \dfrac{a}{\frac{2n\Delta}{n}}$

Where: "a" – Radius of the fiber core
"R_c" – Critical bending radius
"NA" – Numerical aperture of the fiber.

Therefore, from the above equation it can be seen that the major losses at a bend radius of "R_c". But for less light bends, the losses decreases rapidly because of the exponential function. Thus, the evanescent field extends into the cladding due to the bend in the core and exponentially decaying with radial distance. The removal of cladding (U-shaped portion) at a portion of fiber along its length, subject to the higher order mode of the light transmitting to leak out of the fiber and the added bending shape further enhancing the leakage of higher order mode radiations from

the fibers enables an environmental parameter associated with a liquid to be measured with a higher order degree of sensitivity.

A set of liquid mixtures were prepared at different proportions making the total volume equivalent to 20ml, using the combination of Toluene and Acetonitrile and preserved them in separate glass containers with air tight lids. The refractive indices of all the mixtures were determined at various temperatures employing an automatic digital refractometer of model number RX-7000i (Atago make, Japan) at the operating wavelength of 5893Å.

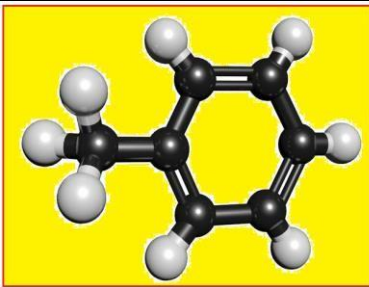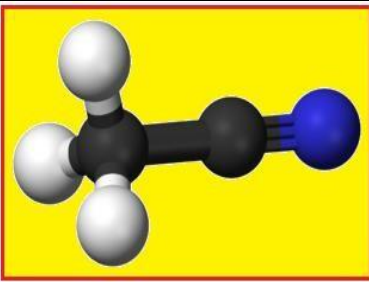**Table.1:** Standard properties of Toluene and Acetonitrile.

Properties	Toluene (C_7H_8)	Acetonitrile (C_2H_3N)
Structure		
CAS No.	108-88-3	75-05-8
Molar Mass (g/mole)	92.141	41.05
Density (kg/m^3)	0.8697×10^3 at 20ºC	0.7822×10^3 at 20ºC
Color	Colourless	Colourless
Refractive index	1.4967 at 20ºC	1.3441 at 20ºC
Melting point	-94.9ºC	-43.8ºC
Boiling point	110.6ºC	81.6ºC

Table.2: Mole fraction of Acetonitrile in Toluene + Acetonitrile chemical mixtures and Refractive indices of mixtures at various temperatures (from 10ºC to 60ºC).

S. No.	Mole fraction of Acetonitrile	Refractive Index at various temperatures										
		10ºC	15ºC	20ºC	25ºC	30ºC	35ºC	40ºC	45ºC	50ºC	55ºC	60ºC
1	0.00000	1.50915	1.50591	1.50171	1.49770	1.49325	1.48974	1.48582	1.48293	1.47795	1.47509	1.47102
2	0.18321	1.48211	1.47795	1.47452	1.47086	1.46675	1.46205	1.45872	1.45495	1.45083	1.44637	1.44283
3	0.33541	1.46009	1.45597	1.45208	1.44795	1.44403	1.44019	1.43623	1.43287	1.42804	1.42413	1.42087
4	0.46386	1.44	1.43	1.43	1.43	1.42	1.42	1.41	1.41	1.41	1.40	1.40

S.No	Mole fraction											
		197	823	426	007	682	187	809	376	007	596	243
5	0.57372	1.42596	1.42187	1.41772	1.41428	1.41049	1.40596	1.40204	1.39804	1.39356	1.39005	1.38604
6	0.66874	1.41075	1.40714	1.40308	1.39914	1.39507	1.39104	1.38705	1.38323	1.37904	1.37543	1.37123
7	0.75175	1.39914	1.39535	1.39153	1.38752	1.38323	1.37985	1.37488	1.37082	1.36713	1.36308	1.35908
8	0.82488	1.38604	1.38258	1.37814	1.37439	1.37018	1.36684	1.36285	1.35875	1.35492	1.35098	1.34696
9	0.88981	1.37712	1.37279	1.36857	1.36478	1.36106	1.35706	1.35268	1.34886	1.34489	1.34086	1.33665
10	0.94783	1.36647	1.36202	1.35804	1.35402	1.35098	1.34643	1.34207	1.33812	1.33407	1.33008	1.32604
11	1.00000	1.35706	1.35304	1.34886	1.34517	1.34108	1.33705	1.33306	1.32903	1.32511	1.32105	1.31721

Maintaining each mixture surrounding the U-shaped glass rod with an immersion depth of 1cm, the light reaching the detector at output end was noted and data was tabulated along with calculated value of mole fraction.

Table.3: Mole fraction of Acetonitrile in Toluene + Acetonitrile chemical mixtures and Output power at various temperatures (from 10°C to 60°C), when depth of immersion of U-shaped glass rod into chemical mixture 1cm.

Output Power when air surrounding the U-shaped glass rod: -24.80dBm (at 30°C)

S.No.	Mole fraction of Acetonitrile	Output Power(dBm) at various temperatures										
		10°C	15°C	20°C	25°C	30°C	35°C	40°C	45°C	50°C	55°C	60°C
1	0.00000	-39.50	-39.20	-39.00	-38.70	-38.33	-38.00	-37.63	-37.37	-36.90	-36.63	-36.30
2	0.18321	-37.3	-37.13	-36.83	-36.67	-36.43	-36.17	-35.83	-35.67	-35.43	-35.2	-34.97
3	0.33541	-35.97	-35.73	-35.6	-35.43	-35.27	-34.93	-34.67	-34.43	-34.07	-33.8	-33.57
4	0.46386	-35.07	-34.8	-34.53	-34.23	-33.97	-33.63	-33.37	-33.03	-32.8	-32.57	-32.4
5	0.57372	-33.9	-33.6	-33.3	-33.0	-32.8	-32.5	-32.3	-32.1	-31.9	-31.6	-31.3

			3	3	7	3	7	7	7	3	7	7
6	0.66874	-32.87	-32.63	-32.43	-32.23	-32	-31.73	-31.43	-31.13	-30.83	-30.6	-30.37
7	0.75175	-32.23	-32.03	-31.77	-31.5	-31.13	-30.87	-30.57	-30.33	-30.07	-29.73	-29.43
8	0.82488	-31.37	-31.07	-30.77	-30.53	-30.3	-30.03	-29.7	-29.4	-29.17	-28.9	-28.63
9	0.88981	-30.7	-30.43	-30.17	-29.87	-29.57	-29.3	-29	-28.77	-28.5	-28.23	-27.6
10	0.94783	-30	-29.63	-29.37	-29.1	-28.9	-28.6	-28.33	-27.8	-27.27	-26.77	-26.2
11	1.00000	-29.3	-29.03	-28.77	-28.53	-28.23	-27.7	-27.2	-26.73	-26.33	-25.67	-25.23

The method of measurement of output powers as a function of temperature corresponding to all the mixtures was repeated by immersing U-shaped glass rod to a depth of 2cm and 3cm sequentially into the liquid.

Table.4: Mole fraction of Acetonitrile in Toluene + Acetonitrile chemical mixtures and Output power at various temperatures (from 10°C to 60°C), when depth of immersion of U-shaped glass rod into chemical mixture 2cm.

S. No.	Mole fraction of Acetonitrile	Output Power(dBm) at various temperatures										
		10°C	15°C	20°C	25°C	30°C	35°C	40°C	45°C	50°C	55°C	60°C
1	0.00000	-42.20	-41.90	-41.50	-41.10	-40.80	-40.50	-40.03	-39.83	-39.40	-39.03	-38.70
2	0.18321	-39.77	-39.40	-39.13	-38.83	-38.53	-38.20	-38.00	-37.77	-37.50	-37.23	-36.87
3	0.33541	-38.07	-37.83	-37.60	-37.33	-37.07	-36.60	-36.20	-35.93	-35.50	-35.10	-34.83
4	0.46386	-36.73	-36.40	-36.03	-35.67	-35.43	-35.03	-34.70	-34.30	-34.10	-33.70	-33.37
5	0.57372	-35.2	-34.9	-34.6	-34.4	-34.1	-33.7	-33.3	-33.2	-32.9	-32.5	-32.2

		7	0	0	0	7	0	3	0	0	7	0
6	0.66874	-34.20	-33.87	-33.53	-33.27	-33.03	-32.67	-32.30	-31.97	-31.63	-31.37	-31.10
7	0.75175	-33.27	-33.07	-32.70	-32.37	-31.97	-31.70	-31.33	-31.07	-30.73	-30.37	-29.97
8	0.82488	-32.20	-31.93	-31.57	-31.30	-31.03	-30.70	-30.33	-30.00	-29.77	-29.50	-29.13
9	0.88981	-31.50	-31.20	-30.87	-30.53	-30.17	-29.90	-29.60	-29.37	-29.10	-28.83	-28.20
10	0.94783	-30.67	-30.27	-29.97	-29.70	-29.50	-29.20	-28.93	-28.50	-27.87	-27.37	-26.80
11	1.00000	-29.90	-29.63	-29.37	-29.13	-28.87	-28.30	-27.73	-27.20	-26.67	-26.17	-25.73

Table.5: Mole fraction of Acetonitrile in Toluene + Acetonitrile chemical mixtures and Output power at various temperatures (from 10ºC to 60ºC), when depth of immersion of U-shaped glass rod into chemical mixture 3cm.

S. No.	Mole fraction of Acetonitrile	Output Power(dBm) at various temperatures										
		10º C	15º C	20º C	25º C	30º C	35º C	40º C	45º C	50º C	55º C	60º C
1	0.00000	-45.23	-44.87	-44.47	-44.07	-43.63	-43.27	-42.87	-42.57	-42.03	-41.80	-41.40
2	0.18321	-42.50	-42.03	-41.73	-41.47	-41.23	-40.87	-40.60	-40.27	-39.77	-39.43	-39.03
3	0.33541	-40.73	-40.37	-40.00	-39.63	-39.27	-38.90	-38.50	-38.17	-37.67	-37.17	-36.77
4	0.46386	-39.07	-38.70	-38.30	-37.87	-37.53	-36.97	-36.53	-36.10	-35.83	-35.40	-34.97
5	0.57372	-37.20	-36.70	-36.30	-36.10	-35.87	-35.40	-34.83	-34.7	-34.40	-34.07	-33.70
6	0.66874	-35.9	-35.6	-35.1	-34.7	-34.5	-34.1	-33.8	-33.4	-33.1	-32.8	-32.5

		0	0	0	7	3	7	0	7	3	7	3
7	0.75175	-34.77	-34.57	-34.23	-33.87	-33.47	-33.20	-32.83	-32.50	-32.17	-31.83	-31.47
8	0.82488	-33.70	-33.40	-33.07	-32.77	-32.43	-32.13	-31.80	-31.43	-31.10	-30.80	-30.43
9	0.88981	-33.00	-32.63	-32.30	-31.97	-31.60	-31.27	-30.93	-30.60	-30.20	-29.70	-29.10
10	0.94783	-32.10	-31.70	-31.37	-31.03	-30.80	-30.37	-29.93	-29.40	-28.73	-28.13	-27.60
11	1.00000	-31.27	-30.97	-30.60	-30.23	-29.83	-29.23	-28.53	-27.93	-27.43	-26.90	-26.40

RESULTS AND DISCUSSION:

In the present experiment, a pair of two chemicals i.e. Toluene and Acetonitrile is chosen for the calibration and development of the sensor. The liquids are taken in different proportions with an incremental/ decremental volumes in steps of 2ml each to prepare the mixtures and the mole fraction of Acetonitrile in the mixture of Toluene + Acetonitrile were determined theoretically. The mole fraction of presence of Acetonitrile in the mixture of Toluene + Acetonitrile, significantly changes the refractive index of the mixture and accordingly the graphical representation between refractive index and mole fraction is presented [fig.-2].

Fig.2: Relation between Mole fraction of Acetonitrile in Toluene + Acetonitrile mixtures and Refractive index.
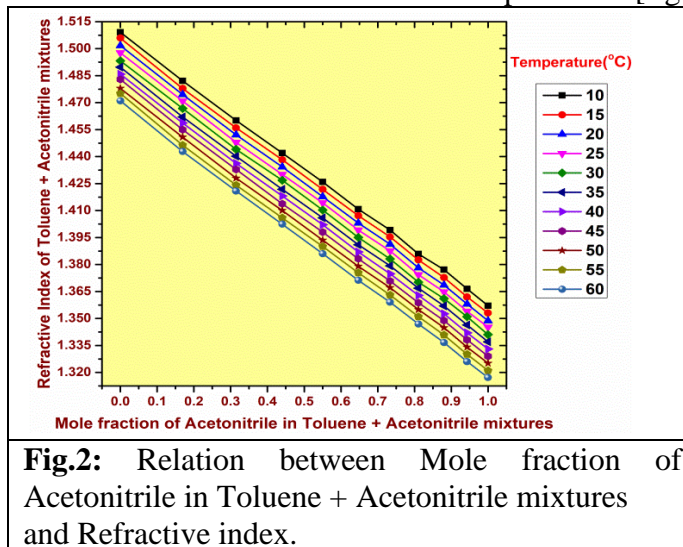
In order to calibrate the sensor, a set of liquids having different indices of refraction ranging from $1.31721n_D$ to $1.50915n_D$ at different temperatures, the mixtures are prepared to have different concentration percentage of Acetonitrile in the mixture of Toluene and Acetonitrile and

the dependence of refractive index of mixtures on the concentration percentage of Acetonitrile in Toluene + Acetonitrile mixtures shown graphically [fig.-3].
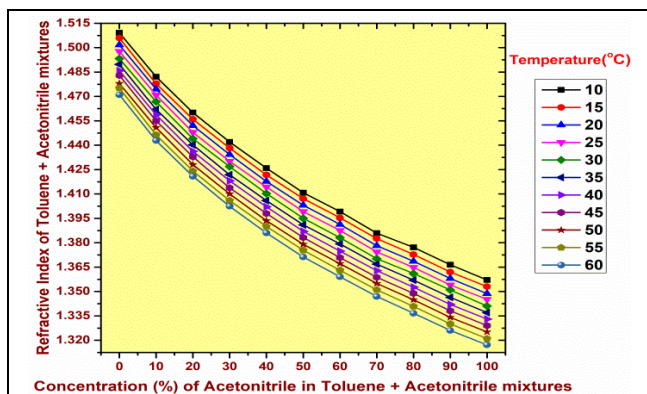

Fig.3: Relation between Concentration (%) of Acetonitrile in Toluene + Acetonitrile mixtures and Refractive index.

The variation of refractive index on temperature was determined with the help of automatic digital refractometer of model number RX-7000i corresponding to each mixture and observed to be linear with the temperature, and the results are plotted in graph [fig.-4].
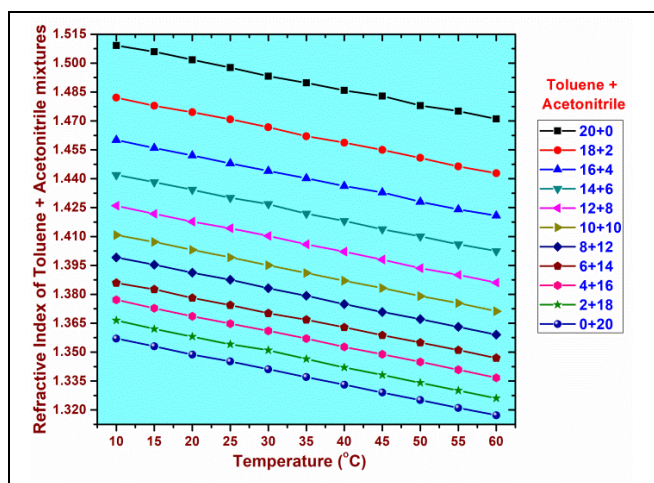
Fig.4: Relation between Temperature and Refractive index of Toluene + Acetonitrile mixtures.

The relationships between the refractive index versus mole fraction of Acetonitrile, and refractive index versus temperature of mixtures are presented in a 3dimentional graph for the quick understating of the variable on the independent parameter [fig.-5].
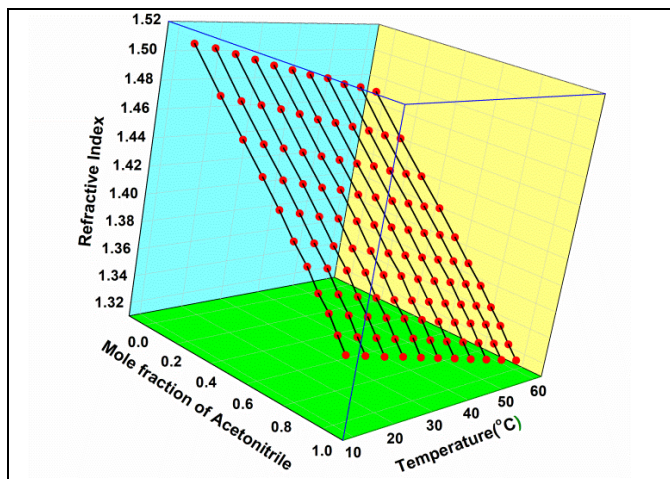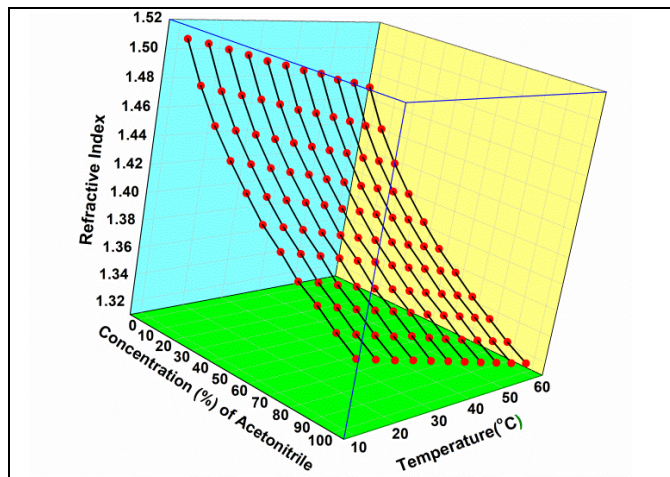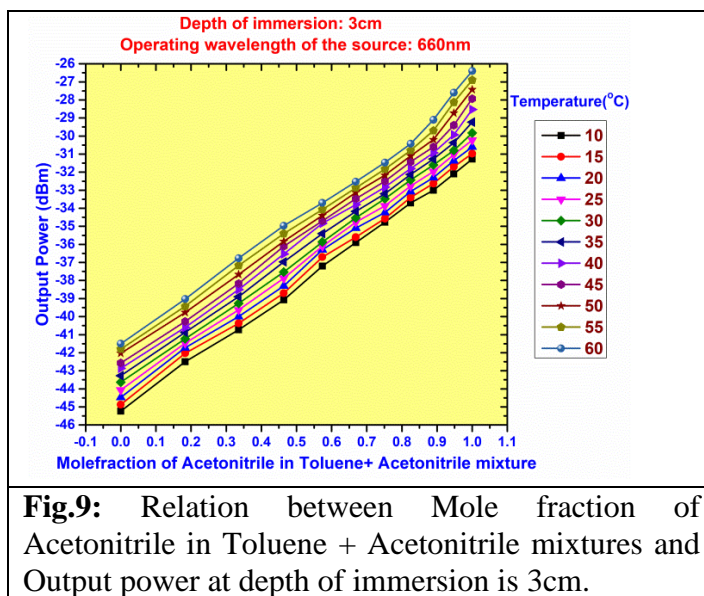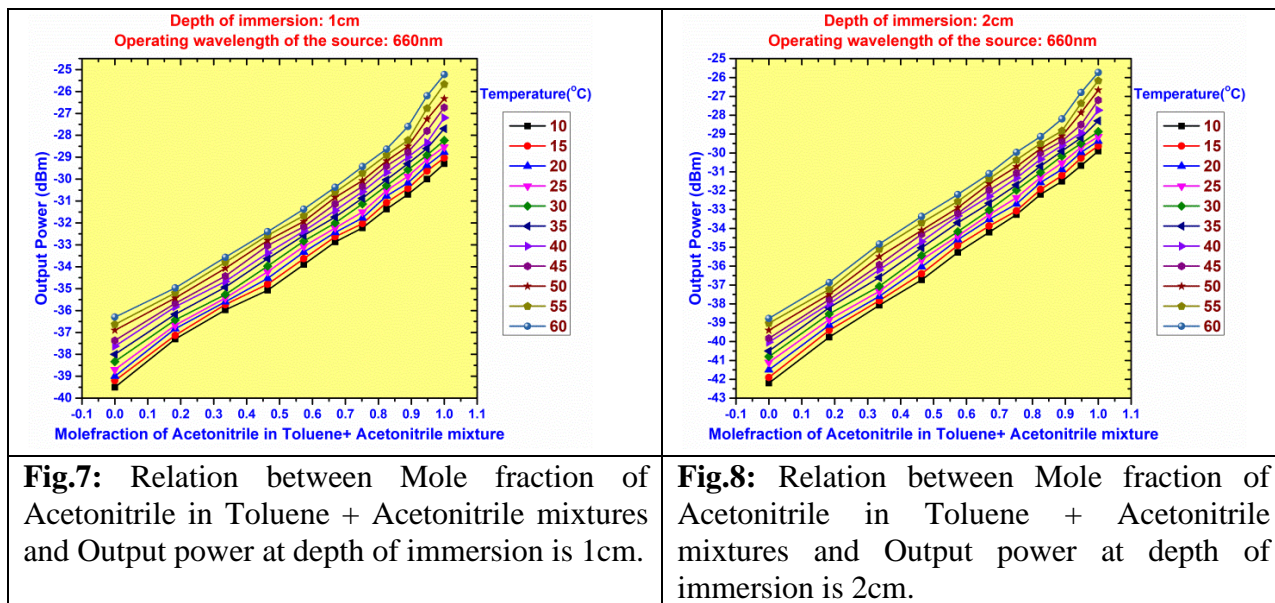
Fig.5: Relation among Mole fraction of Acetonitrile in Toluene + Acetonitrile mixtures, Refractive index and Temperature.

A graph relating temperature dependence on refractive index and concentration percentage of Acetonitrile dependence on refractive index are shown together in 3dimentional graph [fig.-6] and variations are observed that, as the temperature increases, the refractive index decreases and also as the concentration percentage of Acetonitrile in the mixture increases, the refractive index decreases.

Fig.6: Relation among Concentration (%) of Acetonitrile in Toluene + Acetonitrile mixtures, Refractive index and Temperature.

Basically, the relationship between the increase in mole fraction of Acetonitrile in mixture increases, the refractive index of the mixture decreases but from the relationship between refractive index and output power revels that as refractive index of mixture decreases the output power increases, which relationship was shown graphically for the depths of immersions of U-shaped glass rod into the mixtures as 1cm, 2cm and 3cm respectively [fig.7-9].

Fig.7: Relation between Mole fraction of Acetonitrile in Toluene + Acetonitrile mixtures and Output power at depth of immersion is 1cm.	**Fig.8:** Relation between Mole fraction of Acetonitrile in Toluene + Acetonitrile mixtures and Output power at depth of immersion is 2cm.

Fig.9: Relation between Mole fraction of Acetonitrile in Toluene + Acetonitrile mixtures and Output power at depth of immersion is 3cm.

It is well known that, as the temperature of the mixture increases, the refractive index decreases but as the output power depends on refractive index, the increase in temperature results increase in the output power [fig.10-12].
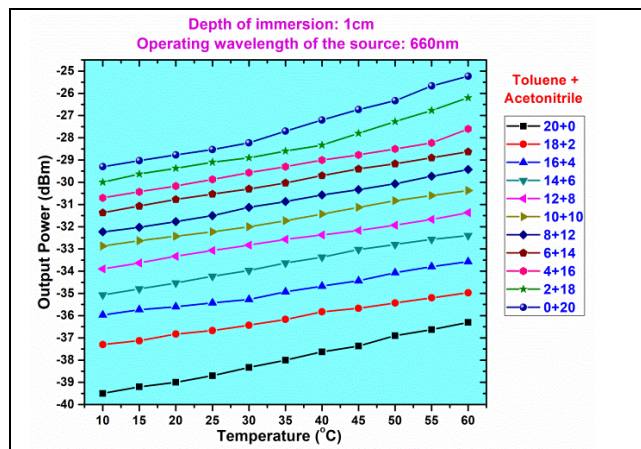
Fig.10: Relation between Temperature and Output power of Toluene + Acetonitrile mixtures at depth of immersion is 1cm
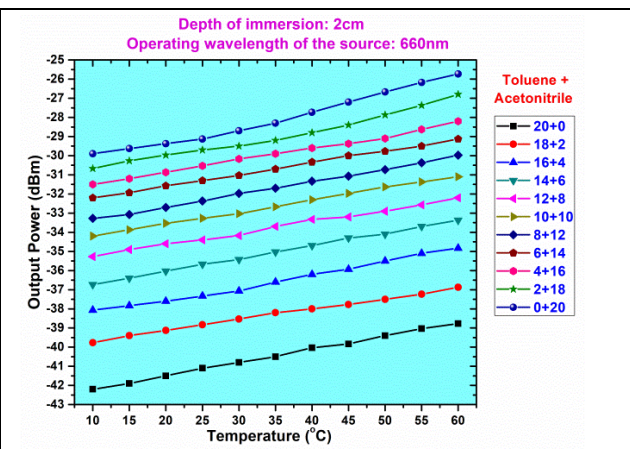
Fig.11: Relation between Temperature and Output power of Toluene + Acetonitrile mixtures at depth of immersion is 2cm
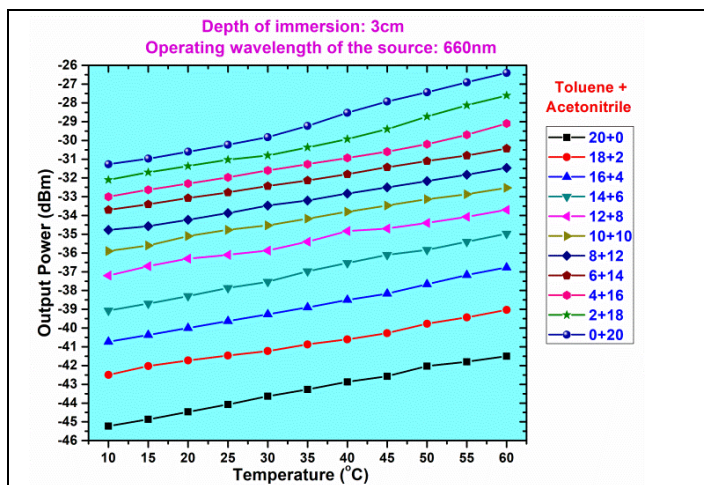

Fig.12: Relation between Temperature and Output power of Toluene + Acetonitrile mixtures at depth of immersion is 3cm

The output power variation with respect to refractive index and related raise in temperature of mixtures are presented in single unified 3dimentional graphs [fig.13-15]. It is observed that refractive index of the mixtures decreases with temperatures resulting a sizable amount of increases in the output power.
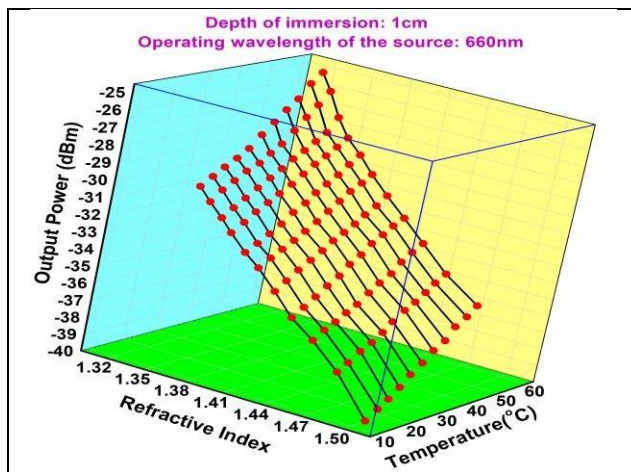
Fig.13: Relation between Refractive index, Output Power and Temperature of Toluene + Acetonitrile at depth of immersion is 1cm
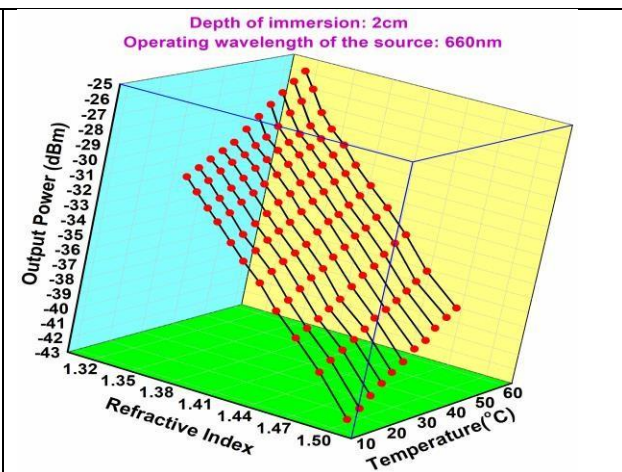

Fig.14: Relation between Refractive index, Output Power and Temperature of Toluene + Acetonitrile at depth of immersion is 2cm
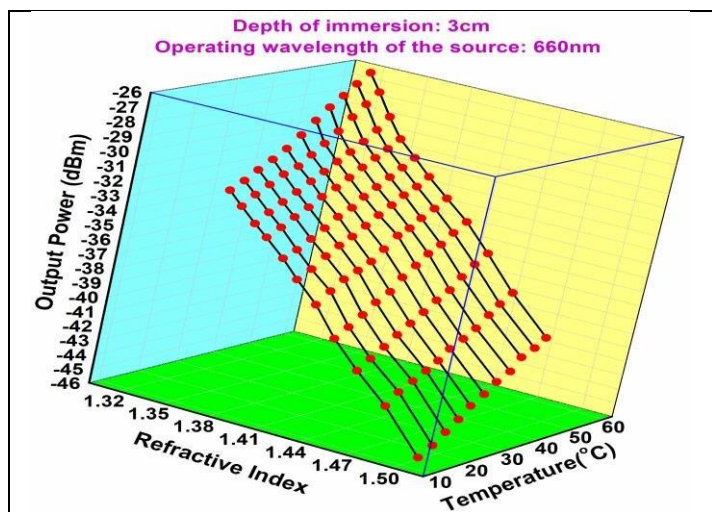

Fig.15: Relation between Refractive index, Output Power and Temperature of Toluene + Acetonitrile at depth of immersion is 3cm

CONCLUSION:

The sensor is calibrated by employing mixtures of Toluene and Acetonitrile, taking in different proportions making the total volume equivalent to 20ml and within the temperature range of 10ºC to 60ºC at the operating wavelength of 660nm. As the length of interaction of measurer (light) with the measurand (liquid mixtures) increases, the sensitivity of the sensor is also increases. This is confirmed by choosing different depth of immersions as 1cm, 2cm and 3cm. This sensor offers all the advantages that are offered by optical fibers in communication and proved to be accurate, rugged, robust, reliable and durable, offering the sensitivities in the order of 10^{-5}. The sensor can be used to measure refractive index of various liquids in the dynamic

refractive index of $1.31721n_D$ to $1.50915n_D$ and in the temperature range of $10^{\circ}C$ to $60^{\circ}C$, operating at the wavelength of 660nm.

REFERENCES:

[1] X. Wang, J. Xu, Y. Zhu, K. L. Cooper, and A. Wang, "All-fused-silica miniature optical fiber tip pressure sensor," Opt. Lett., vol. 31, no. 7, pp. 885–887, 2006.

[2] J. H. Zhu, X. G. Huang, W. Xu, and L. X. Chen, "Plasmonic optical switches based on Mach-Zender interferometer," Phys. Plasmas, vol. 18, no. 7, pp. 72112–72116, 2011.

[3] D. D. Sell, H. C. Casey, and K. W. Wecht, "Concentration dependence of the refractive index for n-and p-type GaAs between 1.2 and 1.8 eV," J. Appl. Phys., vol. 45, no. 6, pp. 2650–2657, Jun. 1974.

[4] B. Gu, M. J. Yin, A. P. Zhang, J. W. Qian, and S. He, "Lowcost high-performance fiber-optic pH sensor based on thin-core fiber modal interferometer," Opt. Exp., vol. 17, no. 25, pp. 22296–22302, 2009.

[5] L. X. Chen, X. G. Huang, J. H. Zhu, G. C. Li, and S. Lan, "Fiber magnetic-field sensor based on nanoparticle magnetic fluid and Fresnel reflection," Opt. Lett., vol. 36, no. 15, pp. 2761–2763, 2011.

[6] K. Y. Lam and M. A. Afromowitz, "Fiber-optic epoxy composite cure sensor. I. Dependence of refractive index of an autocatalytic reaction epoxy system at 850 nm on temperature and extent of cure," Appl. Opt., vol. 34, no. 25, pp. 5635–5638, 1995.

[7] W. Liang, Y. Y. Huang, Y. Xu, R. K. Lee, and A. Yariv, "Highly sensitive fiber Bragg grating refractive indexsensors," Appl. Phys. Lett., vol. 86, no. 15, pp. 151122-1–151122-3, Apr. 2005.

[8] D. Monzón-Hernández and J. Villatoro, "High-resolution refractive index sensing by means of a multiple-peak surface plasmon resonance optical fiber sensor," Sens. Actuators B, vol. 115, no. 1, pp. 227–231, May 2006.

[9] J. F. Ding, A. P. Zhang, L. Y. Shao, J. H. Yan, and S. L. He, "Fiber-taper seeded long-period grating pair as a highly sensitive refractive-index sensor," IEEE Photon. Technol. Lett., vol. 17, no. 6, pp. 1247–1249, Jun. 2005.

[10] G. H. Meeten and A. N. North, "Refractive index measurement of turbid colloidal fluids by transmission near the critical angle," Meas. Sci. Technol., vol. 2, no. 5, pp. 441–447, May 1991.

[11] K. S. Chiang, Y. Liu, M. N. Ng, and X. Dong, "Analysis of etched long-period fiber grating and its response to external refractive index," Electron. Lett., vol. 36, no. 11, pp. 966–967, May 2000.

[12] B. Rothenhausler and W. Knoll, "Surface-plasmon microscopy," Nature, vol. 332, pp. 615–617, Apr. 1988.

[13] X. W. Shu, L. Zhang, and I. Bennion, "Sensitivity characteristics of longperiod fiber gratings," J. Lightw. Technol., vol. 20, no. 2, pp. 255–266, Feb. 2002.

[14] C.-B. Kim and C. B. Su, "Measurement of the refractive index of liquids at 1.3 and 1.5 micron using a fibre optic Fresnel ratio meter," Meas. Sci. Technol., vol. 15, no. 9, pp. 1683–1686, May 1991.

[15 A. Ankiewicz, Pask C. and Snyder A., "Slowly Varying Tapers", J. Opt. Soc. Am. 72, pp. 198-203 (1982).